Acta Materialia 119 (2016) 43–54

Contents lists available at ScienceDirect

Acta Materialia

journal homepage: www.elsevier.com/locate/actamat

Full length article

Thermomechanical processing route to achieve ultrafine grains in low carbon microalloyed steels

P. Gong, E.J. Palmiere, W.M. Rainforth*

Department of Materials Science and Engineering, The University of Sheffield, Sir Robert Hadfield Building, Mappin Street, Sheffield, S1 3JD, UK

ARTICLE INFO

Article history:
Received 7 March 2016
Received in revised form
28 July 2016
Accepted 3 August 2016

Keywords:
Microalloyed steel
Thermomechanical controlled processing
Strain-induced precipitation
Deformation-induced ferrite transformation

ABSTRACT

A new thermomechanical processing route is described for a microalloyed steel, with roughing deformation below the recrystallisation-stop temperature ($T_{5\%}$), followed by a rapid reheat to 1200 °C for 10s, and then finish deformation at the same temperature as the rough deformation. The new route focused on optimising the kinetics of strain-induced precipitation (SIP) and the formation of deformation-induced ferrite transformation (DITF). For comparative purposes, two experimental 0.06 wt% C steels were studied: one with 0.03 wt% Nb (Nb steel), and a second with both 0.03 wt% Nb and 0.02 wt% Ti (Nb–Ti steel). Two processing routes were studied. The first was a conventional route, which consisted of a simulated rough deformation schedule with the final roughing pass taking place at 850 °C, which produced fully unrecrystallised austenite grains during deformation with no strain-induced ferrite formation. The second, new, thermomechanical processing route used the same roughing step, after which the steels were reheated at 10 °C/s to a temperature of 1200 °C, isothermally held for 10s allowing for precipitate dissolution, prior to air cooling to a finishing deformation temperature of 850 °C. This route resulted in DIFT primarily on the prior-austenite grain boundaries. The precipitate solution during the reheat treatment increased the supersaturation of Nb and Ti in the austenite matrix on subsequent cooling, which therefore increased the undercooling due to the increased A_{e3}. The observation of nanoscale cementite in the DIFT supports the view that it formed through a massive transformation mechanism. The volume fraction of SIP after finish deformation was influenced by the supersaturation of microalloy elements in solution during heat treatment. The new process route led to a significant refinement of the final ferrite grain size.

1. Introduction

Thermomechanical controlled processing (TMCP), consisting of controlled hot rolling followed by controlled cooling, is used to maximise the benefits of the microalloy additions present in microalloyed steels [1,2]. The improvement in mechanical properties is due to ferrite grain refinement, which maximises the surface area-to-volume ratio (S_v) of austenite grain boundaries and the deformation band density [3,4]. However, high energy consumption and high rolling loads are a limiting factor for TMCP. Therefore, to address some of the limitations inherent with conventional TMCP, a new thermomechanical processing route has been developed to increase the finish rolling temperature in order to reduce the rolling load and improve the productivity.

Microalloyed steels have been widely utilised because of their enhanced mechanical properties over conventional steels. As is well known, each microalloy addition behaves in a different way; Ti additions enable microstructural refinement by limiting grain coarsening during reheating, while Nb facilitates a high S_v as a result of the strain-induced precipitation of niobium carbides, nitrides or carbonitrides in the austenite. Furthermore, the Nb which remains in solution provides solute drag and through the precipitation of carbides/carbonitrides can subsequently contribute to dispersion hardening either during or after phase transformation [5–7]. Numerous studies of the precipitation kinetics focus on the fully equilibrated isothermal heat treatment in austenite with the retardation of the recrystallisation by precipitation [8] or isothermal austenite to ferrite transformation at the intercritical region [9]. However, there is limited research on the precipitation and dissolution behaviour at the non-fully equilibrated condition of steels containing one or more microalloy element, as well as their influence on the deformation structures.

---

* Corresponding author.
E-mail address: m.rainforth@sheffield.ac.uk (W.M. Rainforth).

http://dx.doi.org/10.1016/j.actamat.2016.08.010
1359-6454/

The $\gamma \rightarrow \alpha$ phase transformation temperature is influenced by the deformation schedule, which therefore determines whether deformation induced ferrite (DIFT) is produced or not. Promoting DIFT has become a favoured method to obtain ultrafine ferrite grains in microalloyed low carbon steels [10–16]. Most of these investigations into DIFT have focused on the effect of chemical composition, the cooling rate and the deformation parameters (strain, strain rate). It has also been observed that a finer prior austenite grain size before deformation increases the extent of DIFT [17]. In the present study, in contrast to the observations of [17], DIFT has been promoted by a larger prior-austenite grain size, promoted by a reheating process between rough and finish deformation, with the aim to refine the final grain size in the transformed product. The mechanism of DIFT formation has been investigated through the role of precipitation, strain and the morphology of the grains as a function of deformation, as well as following isothermal holding after deformation.

2. Experimental procedures

2.1. Material

The materials used in the research consisted of two laboratory cast microalloyed steels containing Nb (designated "Nb steel"), and Nb and Ti (designated "Nb–Ti steel"), which were made by vacuum induction melting and cast into ingots having dimensions 220 mm × 65 mm × 28 mm at ArcelorMittal. The composition of the steels was analysed by Sheffield Testing Laboratories and is listed in Table 1. The ingots were soaked at 1300 °C for 2 h and hot-rolled from 28 mm to 12 mm thick plates in two passes utilising a 2-high fully-instrumented 50 tonne Hille deformation mill with a finishing temperature of 1100 °C followed by an ice water quench. Plane strain compression (PSC) specimens, having a geometry of 60 mm long × 30 mm wide × 10 mm high were machined from the hot rolled and as-quenched plate. PSC testing was performed using the thermomechanical compression (TMC) machine at The University of Sheffield [18]. Samples were reheated to 1100 °C, held for 30s and then force-air cooled to the roughing deformation temperature of 850 °C. This unusually low roughing temperature of 850 °C was chosen as it was below the recrystallisation-stop temperature ($T_{5\%}$) for each steel. Deformation was undertaken in a single pass using a strain of 0.3 with a constant true strain rate of 10 s^{-1}. Immediately after roughing, the steels were rapidly reheated at a rate of 10 °C/s to a temperature of 1200 °C, held for 10s, followed by force-air cooling to 850 °C at a rate of 10 °C/s, with the finishing deformation passes being performed with different deformation parameters. The deformation and heat treatment schedule is illustrated in Fig. 1. Condition A was deformed to a strain of 0.3 at a strain rate of 10/s, and immediately quenched (designated "0s" as there was no hold at temperature). Condition B underwent the same deformation schedule as condition A, but with a 10s hold prior to quenching. Condition C underwent the same thermomechanical schedule as condition B, but then received an additional strain of 0.3 at a strain rate of 10/s followed by an immediate water quench. This material had therefore received a total finish deformation strain of 0.6. Finally, condition D received the same thermomechanical schedule as condition C, but with a final 10s hold prior to water quenching.

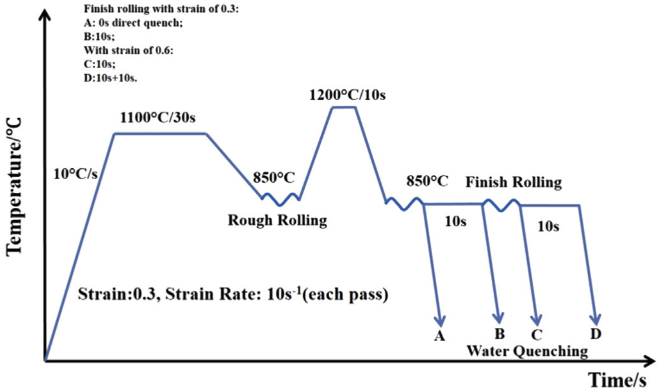

Fig. 1. Schematic of the thermomechanical cycles used and nomenclature used for each condition.

Table 1
Chemical composition of the experimental steels (wt%).

	C	Si	Mn	Cr	Ni	Nb	Ti	N	P
Nb steel	0.067	0.11	0.77	0.01	0.02	**0.03**	<**0.01**	0.0058	0.016
Nb–Ti steel	0.065	0.11	0.77	0.01	0.02	**0.03**	**0.02**	0.0062	0.016

The significance of the bold values is that these two alloying elements represent the microalloying elements present in the two steels, which indeed distinguishes one steel from the other.

2.2. Grain size and microstructure

Longitudinal specimens were prepared for metallographic examination using standard techniques. The polished specimens were etched in a solution of saturated picric acid at 60 °C to reveal the prior-austenite grain boundaries. The average austenite grain size was measured using the linear intercept method (ASTM E-112) by optical microscopy (OM). Scanning electron microscopy (SEM) was used to observe the microstructures of ferrite and martensite, which was etched using a 2% nital solution for approximately 5–10s. Electron backscatter diffraction (EBSD) was used to measure the final sub-grain size after finish deformation from the Nb–Ti steel. Samples for EBSD were prepared by the same method as the SEM samples. The acceleration voltage of 20 kV and an emission current of around 80 μA were chosen with the step size of 300 nm. The minimum misorientation angle that defines a grain boundary was set to 2°. Misorientation angles between 2° and 15° were regarded as low-angle grain boundaries, while those larger than 15° were designated high-angle grain boundaries.

2.3. Precipitate analysis

Transmission electron microscopy (TEM) was carried out to identify the strain-induced precipitation. Carbon extraction replicas were prepared in the standard manner using a light 2% nital etch. Subsequent thin foils were electropolished using an electrolyte solution of 5% perchloric acid, 35% butoxyethanol and 60% methanol. Extraction replica samples and thin foil samples were examined in FEI Tecnai T20 and JEOL 2010F TEM. The particle diameter distribution of precipitates was measured for each sample, with around 200 particles counted in each case, with quantitative image analysis being performed using Image J software. Additionally, chemical analysis of the precipitates was conducted using an Oxford instruments energy dispersive X-ray spectroscopy (EDX) detector (Oxford Instruments, Oxford, UK) and electron energy loss spectroscopy (EELS) analysis, using a Gatan GIF. The measurement of the sample thickness was carried also carried out using EELS. This was estimated from the low energy region of the spectrum, given by Eq. (1) [19,20]:

$$t = \lambda \ln(I_t/I_0) \tag{1}$$

where t represents the thickness of material; λ is the mean free